J Mol Model (2009) 15:1329–1336
DOI 10.1007/s00894-009-0496-z

ORIGINAL PAPER

Structures and aromaticity of $X_2Y_2^-$ (X = C, Si, Ge and Y = N, P, As) anions

Wen Guo Xu · Yuan Chun Zhang · Shi Xiang Lu · Rui Chun Zhang

Received: 28 January 2009 / Accepted: 19 March 2009 / Published online: 22 April 2009

Abstract The equilibrium geometries, total energies, and vibrational frequencies of anions $X_2Y_2^-$ (X = C, Si, Ge and Y = N, P, As) are theoretically investigated with density functional theory (DFT) method. Our calculation shows that for $C_2N_2^-$ species, the D_{2h} isomer is the most stable four-membered structure, and for other species the C_{2v} isomer in which two X atoms are contrapuntal is the most stable structure at the B3LYP/6-311 +G* level. Wiberg bond index (WBI) and negative nucleus-independent chemical shift (NICS) value indicate the existence of delocalization in stable $X_2Y_2^-$ structures. A detailed molecular orbital (MO) analysis further reveals that stable isomers of these species have strongly aromatic character, which strengthens the structural stability and makes them closely connected with the concept of aromaticity.

Keywords DFT calculation · Geometric structure · Molecular orbital · Nucleus-independent chemical shift

Introduction

In the early 19th century, the term "aromatic" was first used to describe organic substances with a pleasant smell, and then to designate a class of chemically related compounds [1]. Traditional arguments about the concept of aromaticity include the following: (i) a regular, delocalized structure involving C-C bonds of equal length, each with partial double-bond character, (ii) enhanced thermodynamic stability, and (iii) reduced reactivity as compared to nonaromatic conjugated hydrocarbons. On the contrary, antiaromatic and nonaromatic compounds show different characteristics. Up to now, although the definition of this concept is still loose, the concept of aromaticity (or its antiaromaticity counterpart) plays an important role in understanding chemical and physical properties of ring-containing conjugated hydrocarbons and many other systems. Especially, in the last two decades, aromaticity becomes a popular topic again. It may be noted that when the concept of aromaticity and antiaromaticity was extended from organic to inorganic molecule and other clusters [2–31], analytical criterion for aromaticity achieved a corresponding progress. Generally speaking, the researcher utilizes structural properties (equalization of bond lengths), magnetic properties (existence of ring currents) as well as spectroscopic features to depict this special concept. It is noteworthy that the proposition of NICS method [32] based on magnetic shielding in 1996 has expanded the applied range for the concept of aromaticity effectively.

In recent years, aromaticity of ring clusters like Al_4^{2-}, Ga_4^{2-}, In_4^{2-}, Hg_4^{6-}, Al_3^-, Ga_3^- units and their derivatives were given much attention [33–36]. Very recently, Satpati and Sebastian investigated BH/C-capped Al_4Li_4 species, and showed the increase of aromaticity for these species [37].

Considering the contribution of different atom on the stability and aromaticity, we investigated $X_2Y_2^-$ (X = C, Si, Ge and Y = N, P, As) species by geometric structures analysis, natural bond orbital (NBO) analysis, nucleus-independent chemical shifts (NICS) and molecular orbital (MO) analysis. Apart from this aspect, the calculation offers some information for a similar subject including the research about C_2N_2 or other neutral X_2Y_2 species. Taking C_2N_2 for example, it was first synthesized in 1815 [38], but the first synthesis of its isomer CNCN was reported in 1988

W. G. Xu · Y. C. Zhang · S. X. Lu · R. C. Zhang (✉)
Institute of Chemical Physics, Beijing Institute of Technology, Beijing 100081, China
e-mail: bitycz@bit.edu.cn

[39]. In this process, the theoretical study plays an important role. Therefore, we hope this research can provide a significant reference for the preparation of related substances with X_2Y_2 species. Moreover, the research shows that π aromaticity arising from delocalized π orbitals strengthens the structural stability and makes stable isomers closely connected with the concept of aromaticity. Certainly, that strongly exhibits the reasonable application of aromatic criterion from organic to inorganic species.

Computational methods

In the current work, all calculations were performed using the Gaussian 03 [40] program. The DFT methods employed in this paper include B3LYP (B3 and the non-local correlation of Lee, Yang, and Parr) and B3PW91 (Becke's three-parameter hybrid functional and Perdew and Wang's 1991 gradient-corrected correlation functional) [41–43]. In addition, the geometries were optimized with Møller-Plesset second order perturbation theory (MP2) method [44, 45]. The 6-311 +G* basis set was used in the whole calculation, which is a split-valence triple-zeta plus polarization basis set augmented with diffuse functions. The natural bond orbital [46] (NBO) analysis was carried out to provide insight into the bonding nature for these species. NICS values for stable $X_2Y_2^-$ species were also calculated using the GIAO [47] -B3LYP method with the corresponding basis set. Molecular orbitals (MOs) for stable $X_2Y_2^-$ clusters were calculated with the corresponding basis set with B3LYP method. All MO pictures were made using the MOLDEN 4.1 program.

Results and discussion

The optimized geometric structures of $X_2Y_2^-$ (X = C, Si, Ge and Y = N, P, As) species are shown in Fig. 1. Total energies and zero-point energy (ZPE) of all species are summarized in Table 1. The calculated vibrational frequencies and IR spectroscopic intensity are listed in Table 2. NICS values in different observation points are given in Table 3 and some important MO pictures are exhibited in Fig. 2.

Geometric structures

In DFT calculation, all possible structures of the $X_2Y_2^-$ (X = C, Si, Ge and Y = N, P, As) species were optimized with B3LYP, B3PW91 and MP2 method. The research results show that each species has three four-membered ring structures, namely, a D_{2h} isomer and two C_{2v} isomers.

From Table 1, we can see that for three isomers of each $X_2Y_2^-$ species, the total energy with the B3LYP method is lower than that with the B3PW91 and MP2 method. Taking the D_{2h} isomer of $C_2N_2^-$ species for example, the total energy with B3LYP method is lower than that with B3PW91 method by 50.2 kcal mol^{-1}, with MP2 method by 320.5 kcal mol^{-1}. Meanwhile, for $C_2N_2^-$ species, the D_{2h} isomer has a lower two energy compared to the other two C_{2v} isomers. However, for other $X_2Y_2^-$ species, the total energy of C_{2v} isomer in which two X atoms are contrapuntal is the lowest. As for the most stable isomer of each $X_2Y_2^-$ species except for $C_2N_2^-$ species, the structure also shows a certain difference. From Table 2, we can find that the most stable and less stable isomers of $X_2Y_2^-$ species have a real vibrational frequency with the B3LYP method, and several isomers with the highest total energy have imaginary frequencies.

Moreover, from Fig. 1, we can find that the four X-Y bond lengths of the most stable and less stable $X_2Y_2^-$ structure are equal, which provides the structural criteria of aromaticity. In addition, according to NBO analysis, we also studied the Wiberg bond index (WBI) of the most stable and less stable $X_2Y_2^-$ isomers. This result tallies closely with the following NICS and MO analysis. We find that for the most stable $C_2N_2^-$ species, the WBI of C-N is 1.17. For the most stable $C_2P_2^-$ and $C_2As_2^-$ species, the WBIs of C-C are 1.39 and 1.73, respectively. For the most stable $X_2Y_2^-$ (X = Si, Ge and Y = N, P, As) species, the WBIs of X-Y are in the range of 1.16–1.18. For less stable $X_2Y_2^-$ species, the WBIs also display an analogous range. For instance, the WBIs of X-Y for less stable $X_2Y_2^-$ (X = C, Si, Ge and Y = P, As) species is 1.06–1.19. It is obvious that these ranges are located between the standard values of single-bond (1.0) and double-bond (2.0), which greatly indicates the existence of delocalization in stable $X_2Y_2^-$ structures. In terms of the above analysis, we can think that for $C_2N_2^-$ species, the D_{2h} isomer is the most stable four-membered structure, and for other species the C_{2v} isomer in which two X atoms are contrapuntal is the most stable structure. What is more, these stable $X_2Y_2^-$ isomers possess a strongly aromaticity nature.

Nucleus-independent chemical shifts (NICS)

In our present work, we first calculated NICS (0.0), NICS (0.5) and NICS (1.0) values of the most stable $X_2Y_2^-$ (X = C, Si, Ge and Y = N, P, As) by placing a ghost atom at or above the geometrical centers for these species. From Table 3, we can clearly see that all calculated NICS values of the most stable $X_2Y_2^-$ species are negative. According to NICS aromatic criterion that a negative NICS value denotes aromaticity, a positive value implies antiaromaticity and

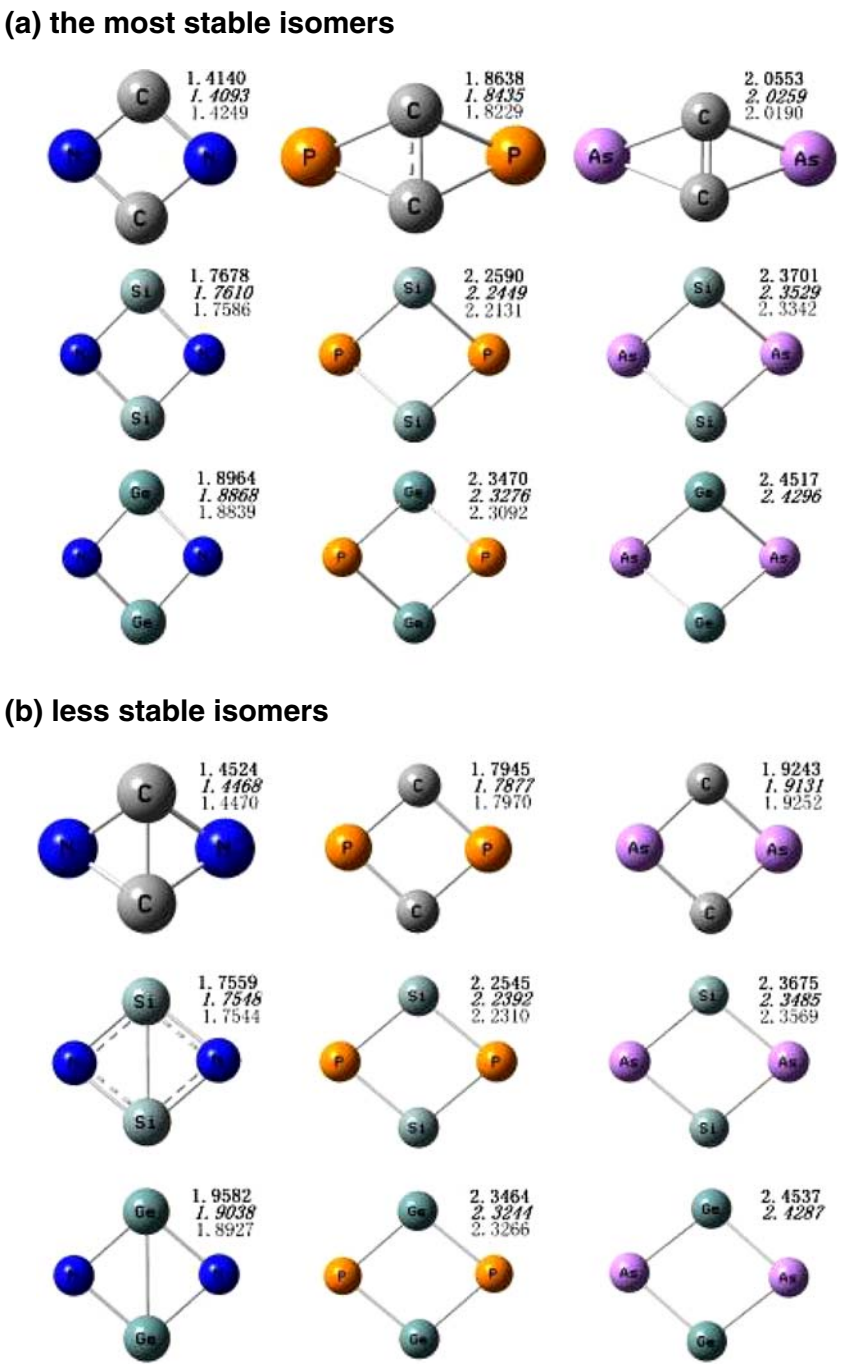

Fig. 1 Optimized geometries of $X_2Y_2^-$ (X = C, Si, Ge and Y = N, P, As) species with the B3LYP (bold), B3PW91 (italic) and MP2 methods. Bond lengths are given in Å, (a) the most stable isomers; (b) less stable isomers; (c) the third isomers

NICS value fluctuating around zero indicates nonaromaticity, these negative NICS values powerfully show the existence of aromaticity in the most stable $X_2Y_2^-$ structures. When we pay more attention to the NICS results of the most stable $X_2Y_2^-$ species, many interesting features can be found. For the most stable $C_2N_2^-$, $C_2P_2^-$ and $C_2As_2^-$ species, NICS (0.5) value is the smallest. For example, NICS (0.5) value (−40.9) of $C_2As_2^-$ species is nearly 4 times smaller than that (−9.9) of C_6H_6 (D_{6h}). However, for Si $_2P_2^-$, $Si_2As_2^-$ and $Ge_2P_2^-$ species, NICS (0.0) value is the smallest. And for $Ge_2N_2^-$ and Ge_2 As_2^- species, NICS (1.0) value is the smallest. To a certain extent, these differences indicate that the position where NICS value is the most suitable to be used to evaluate the aromaticity of these structures is different. In addition, for the most stable $C_2N_2^-$ species, its calculated NICS values give a ordering of (0.5) < NICS (1.0) < NICS (0.0). For the most stable $C_2P_2^-$ and $C_2As_2^-$ species, their NICS ordering is (0.5) < NICS (0.0) < NICS (1.0). Meanwhile, for the most stable $Si_2N_2^-$, $Si_2P_2^-$, $Si_2As_2^-$ and $Ge_2P_2^-$ species, their NICS values give an ordering of NICS (0.0) < NICS (0.5) < NICS (1.0). For the most stable $Ge_2N_2^-$ and $Ge_2As_2^-$ species,

Fig. 1 (continued)

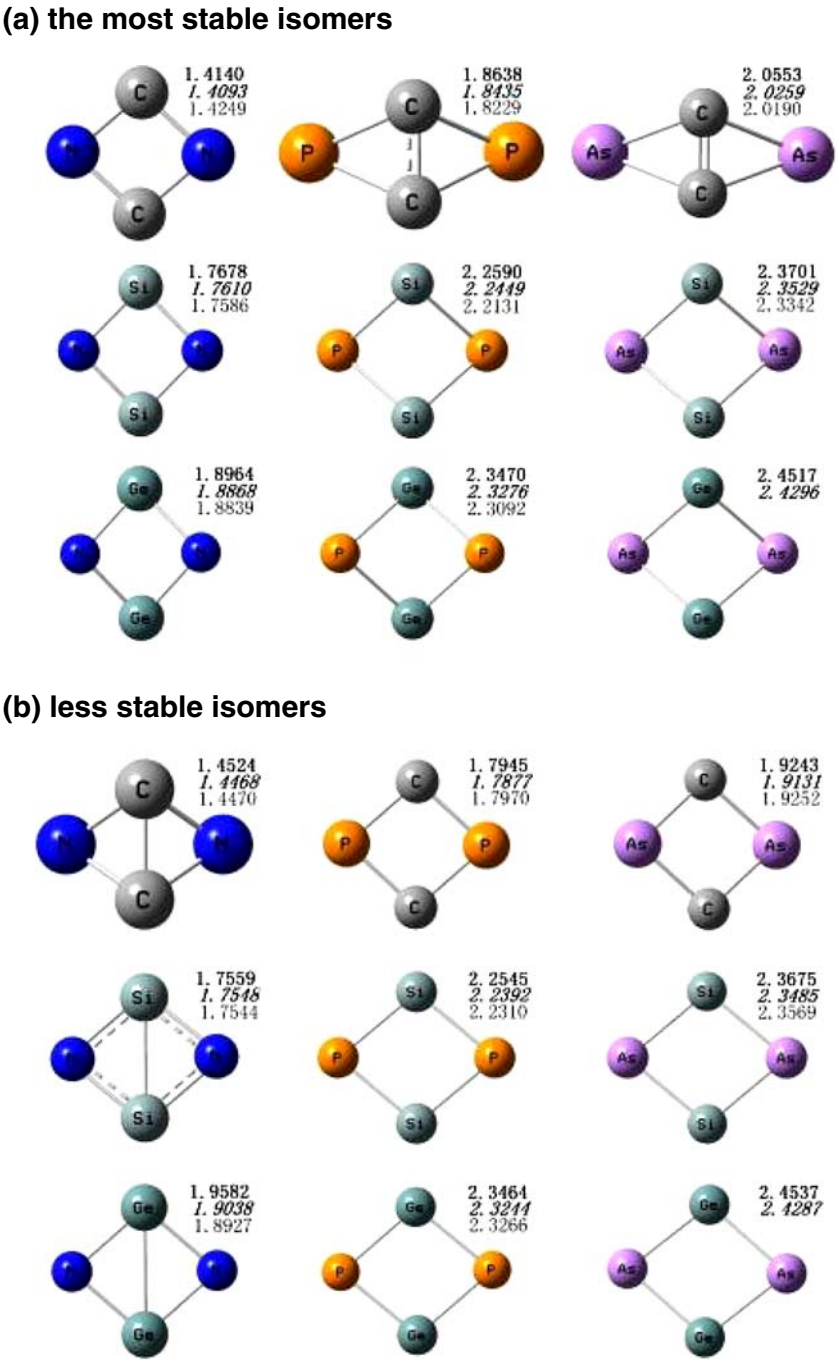

their NICS ordering is NICS (1.0) < NICS (0.5) < NICS (0.0). These NICS ordering differences display the change of aromatic size for the most stable $X_2Y_2^-$ species. Moreover, for the most sable $C_2N_2^-$ species, when the C atom is replaced by Si or Ge atoms, their NICS (0.0) and NICS (0.5) values ordering is $Si_2N_2^- < C_2N_2^- < Ge_2N_2^-$. However, their NICS (1.0) values become smaller. As tabulated in Table 3, when the N atom of the most stable $C_2N_2^-$ species is replaced by P or As atoms, their NICS (0.0) and NICS (1.0) values ordering is $C_2P_2^- < C_2As_2^- < C_2N_2^-$. And their NICS (0.5) values become smaller. The above analysis maybe shows that the same group element has an important effect on aromaticity in the corresponding position for these stable structures.

In order to understand the effect of aromaticity in $X_2Y_2^-$ species more sufficiently, we also present NICS values of less stable isomers in the above positions. From Table 3, we can notice that for $C_2P_2^-$, $C_2As_2^-$ and $Ge_2As_2^-$ species,

Table 1 Total energies (E) and zero-point energies (ZPE) for $X_2Y_2^-$ (X = C, Si, Ge and Y = N, P, As) species

Species		B3LYP			B3PW91			MP2	
		E[a]	ZPE[b]		E[a]	ZPE[b]		E[a]	ZPE[b]
$C_2N_2^-$	a1, D_{2h}	−185.525088	7.20	a1′, D_{2h}	−185.445085	7.32	a1″, D_{2h}	−185.014268	11.8
	a2, C_{2v}	−185.501752	6.82	a2′, C_{2v}	−185.425510	7.12	a2″, C_s	−184.980822	10.2
	a3, C_{2v}	−185.480666	7.92	a3′, C_{2v}	−185.476892	7.25	a3″, C_2	−185.046897	7.84
$C_2P_2^-$	b1, C_{2v}	−758.817085	4.99	b1′, C_{2v}	−758.686566	5.22	b1″, C_{2v}	−757.535938	5.60
	b2, D_{2h}	−758.805583	5.06	b2′, C_s	−758.671371	5.15	b2″, C_s	−757.434571	15.0
	b3, C_{2v}	−758.805563	5.07	b3′, C_{2v}	−758.686512	4.38	b3″, C_{2v}	−757.518148	9.99
$C_2As_2^-$	c1, C_{2v}	−4547.850876	4.29	c1′, C_{2v}	−4547.770325	4.47	c1″, C_{2v}	−4544.381194	4.79
	c2, D_{2h}	−4547.815288	4.06	c2′, C_s	−4547.734192	4.17	c2″, C_s	−4544.349464	8.53
	c3, C_{2v}	−4547.815228	4.06	c3′, C_{2v}	−4547.778719	3.90	c3″, C_{2v}	−4544.368097	15.76
$Si_2N_2^-$	d1, C_{2v}	−688.486556	4.71	d1′, C_{2v}	−688.334906	4.82	d1″, D_{2h}	−687.162155	5.13
	d2, D_{2h}	−688.432531	5.52	d2′, D_{2h}	−688.334676	4.66	d2″, C_{2v}	−687.162156	5.12
	d3, C_{2v}	−688.417867	3.92	d3′, C_{2v}	−68.3086268	4.01	d3″, C_{2v}	−687.155804	6.65
$Si_2P_2^-$	e1, C_{2v}	−1261.814824	2.92	e1′, C_{2v}	−1261.617932	3.04	e1″, C_{2v}	−1259.726932	3.26
	e2, D_{2h}	−1261.774889	2.74	e2′, D_{2h}	−1261.578496	2.83	e2″, D_{2h}	−1259.676972	19.1
	e3, C_{2v}	−1261.759827	2.36	e3′, C_{2v}	−1261.562261	2.43	e3″, C_{2v}	−1259.671115	4.01
$Si_2As_2^-$	f1, C_{2v}	−5050.858831	2.34	f1′, C_{2v}	−5050.715158	2.44	f1″, C_{2v}	−5046.598862	2.63
	e2, D_{2h}	−5050.819970	2.16	f2′, D_{2h}	−5050.676504	2.23	f2″, D_{2h}	−5046.570518	5.15
	f3, C_{2v}	−5050.804943	1.81	f3′, C_{2v}	−5050.660323	1.83	f3″, C_{2v}	−5046.545081	3.09
$Ge_2N_2^-$	g1, C_{2v}	−4263.541503	3.88	g1′, C_{2v}	−4263.431726	3.98	g1″, C_{2v}	−4260.029552	9.02
	g2, D_{2h}	−4263..450668	3.06	g2′, C_{2v}	−4263.367392	2.89	g2″, D_{2h}	−4259.959478	4.40
	g3, C_{2v}	−4263.409788	3.84	g3′, C_{2v}	−4263.405242	2.38	g3″, C_{2v}	−4259.827895	3.34
$Ge_2P_2^-$	h1, C_{2v}	−4836.863532	2.25	h1′, C_{2v}	−4836.707888	2.35	h1″, C_{2v}	−4832.566320	2.50
	h2, D_{2h}	−4836.819159	2.01	h2′, D_{2h}	−4836.663688	2.10	h2″, D_{2h}	−4832.521437	8.35
	h3, C_{2v}	−4836.819139	2.01	h3′, C_{2v}	−4836.657364	1.97	h3″, C_{2v}	−4832.518162	3.03
$Ge_2As_2^-$	i1, C_{2v}	−8625.944637	1.64	i1′, C_{2v}	−8625.807031	1.72	i1″, D_{2h}	-	-
	i2, D_{2h}	−8625.867980	1.46	i2′, D_{2h}	−8625.764613	1.53	i2″, C_{2v}	-	-
	i3, C_{2v}	−8625.859082	1.33	i3′, C_{2v}	−8625.754992	1.39	i3″, C_{2v}	-	-

[a] Total energies in Hartree

[b] Zero-point energies in kcal mol^{-1}

calculated NICS values in corresponding position become larger compared to the most stable structures. For example, NICS (0.0) value (−36.4) of the most stable structure for $C_2P_2^-$ species is nearly eight times smaller than that (−4.3) of less stable isomer. For another example, NICS (0.5) value (−40.9) of the most stable structure for $C_2As_2^-$ species is nearly seven times smaller than that (−5.7) of the less stable isomer. These large NICS values in the less stable isomers answer to the lower stability compared to the most stable structure. It is noteworthy that NICS value of the less stable isomer in the corresponding position is smaller than that of the most stable structure for $C_2N_2^-$ species. For two isomers of other $X_2Y_2^-$ species, the change of NICS value in the corresponding position is not identical. For $Si_2P_2^-$, $Si_2As_2^-$ and $Ge_2P_2^-$ species, on the one hand, NICS (0.0) value of less stable isomer becomes larger compared to the most stable structure, and on the other, NICS (0.5) and NICS (1.0) values become smaller. However, for the less stable isomer of $Ge_2N_2^-$ species, NICS (0.0) value becomes smaller, and NICS (0.5) and NICS (1.0) values become larger compared to the most stable isomer. These NICS changes perhaps show that although NICS value can show the aromaticity, it is not the only aspect in exploring the structural stability for stable $X_2Y_2^-$ species. From the above analysis, we can clearly find that organic species differs much from inorganic species in the aromatic nature.

Molecular orbital (MO) analysis

From Fig. 2a, we can see that the HOMO ($1b_{1g}$) and HOMO-2 ($1b_{2g}$) of the most stable $C_2N_2^-$ are two

Table 2 Calculated vibrational frequencies (in cm^{-1}) and IR spectroscopic intensity (in km mol^{-1}) for $X_2Y_2^-$ (X = C, Si, Ge and Y = N, P, As) at the B3LYP/6-311 +G* level of theory

Species		B3LYP					
		ω_1	ω_2	ω_3	ω_4	ω_5	ω_6
$C_2N_2^-$	a1, D_{2h}	357(78)	602(94)	848(1)	979(0)	1001(0)	1240(0)
	a2, C_{2v}	358(204)	649(0)	653(6)	811(1)	1016(1)	1282(2)
$C_2P_2^-$	b1, C_{2v}	239(7)	383(76)	397(4)	648(0)	718(3)	1103(30)
	b2, D_{2h}	215(0)	483(0)	509(14)	709(13)	798(0)	830(0)
$C_2As_2^-$	c1, C_{2v}	127(3)	203(55)	331(18)	493(0)	524(3)	1321(19)
	c2, D_{2h}	166(2)	296(0)	400(13)	584(10)	672(0)	721(0)
$Si_2N_2^-$	d1, C_{2v}	306(63)	442(4)	540(223)	588(8)	661(0)	756(2)
	d2, D_{2h}	365(37)	539(14)	585(0)	605(0)	788(0)	978(516)
$Si_2P_2^-$	e1, C_{2v}	209(1)	254(1)	272(0)	413(4)	424(22)	472(9)
	e2, D_{2h}	144(9)	258(0)	285(12)	363(3)	425(0)	443(0)
Si_2As^-	f1, C_{2v}	146(0)	192(0)	232(0)	328(1)	347(5)	389(4)
	f2, D_{2h}	108(1)	161(0)	230(11)	294(5)	355(0)	362(0)
$Ge_2N_2^-$	g1, C_{2v}	226(5)	338(14)	363(0)	490(17)	631(215)	663(5)
	g2, D_{2h}	233(39)	267(0)	358(0)	385(7)	533(0)	595(1138)
$Ge_2P_2^-$	h1, C_{2v}	153(1)	185(3)	209(0)	324(25)	324(10)	377(8)
	h2, D_{2h}	109(15)	172(0)	210(3)	258(0)	306(0)	353(0)
$Ge_2As_2^-$	i1, C_{2v}	115(0)	135(0)	157(0)	231(4)	239(6)	271(3)
	i2, D_{2h}	78(3)	127(0)	151(3)	190(2)	231(0)	248(0)

antibonding MOs, which are primarily formed from the out-of-plane p orbital. However, the former is formed from C(1) and C(2) atoms, and the latter is formed from N(3) and N (4) atoms. The HOMO-1 ($2b_{2u}$), HOMO-3 ($2b_{1u}$) and HOMO-7 ($1b_{3g}$) are three partially bonding MOs, which are primarily formed in-plane p orbital of four atoms of this species. The HOMO-4 ($3a_g$), HOMO-5 ($2a_g$), HOMO-8 ($1b_{2u}$) and HOMO-9 ($1b_{1u}$) are also four partially bonding MOs, but they are primarily formed s and in-plane p orbital of four atoms of this species. The HOMO-6 ($1b_{3u}$) is a delocalized bonding MO, which is primarily formed from the out-of-plane p orbital of C(1), C(2), N(3), and N(4) atoms. The HOMO-10 ($1a_g$) is a bonding MO, which is primarily formed from the s orbital of the four atoms of $C_2N_2^-$ (D_{2h}). As a delocalized π MO, the HOMO-6 ($1b_{3u}$) has two π electrons, satisfies the (4n+2) Huckel rule, and renders π aromaticity to $C_2N_2^-$ (D_{2h}) species.

Table 3 Calculated NICS values (in ppm) for $X_2Y_2^-$ (X = C, Si, Ge and Y = N, P, As) species at the B3LYP/6-311 +G* level of theory

Species		B3LYP		
		NICS(0.0)	NICS(0.5)	NICS(1.0)
C_6H_6	D_{6h}	−7.9	−9.9	−10.4
$C_2N_2^-$	a1, D_{2h}	−7.7	−11.5	−9.4
	a2, C_{2v}	−34.9	−38.0	−23.9
$C_2P_2^-$	b1, C_{2v}	−36.4	−38.2	−24.1
	b2, D_{2h}	−4.3	−7.4	−8.1
$C_2As_2^-$	c1, C_{2v}	−33.3	−40.9	−23.7
	c2, D_{2h}	−2.5	−5.7	−7.1
$Si_2N_2^-$	d1, C_{2v}	−24.7	−24.6	−12.4
	d2, D_{2h}	−7.2	−7.0	−5.2
$Si_2P_2^-$	e1, C_{2v}	−6.8	−4.1	−3.5
	e2, D_{2h}	−5.6	−6.2	−6.0
$Si_2As_2^-$	f1, C_{2v}	−7.7	−5.3	−4.1
	f2, D_{2h}	−5.0	−5.6	−5.7
$Ge_2N_2^-$	g1, C_{2v}	−5.2	−10.3	−13.2
	g2, D_{2h}	−7.2	−7.0	−5.2
$Ge_2P_2^-$	h1, C_{2v}	−9.3	−6.5	−5.3
	h2, D_{2h}	−6.5	−6.6	−5.8
$Ge_2As_2^-$	i1, C_{2v}	−5.5	−7.5	−9.7
	i2, D_{2h}	−5.3	−5.7	−5.3

In addition, from Fig. 2b, we also can find that there are delocalized bonding MO in the most stable structure for other $X_2Y_2^-$ species. For the most stable $C_2P_2^-$ and $C_2As_2^-$ species, the HOMO-6 ($3a_1$) is a partially bonding MO and delocalized on C(1)–C(2) bond. For the most stable $Si_2N_2^-$ species, the HOMO-5 ($3a_1$) is a partially bonding MO and delocalized on N(3)–N(4) bond. For the most stable $Si_2P_2^-$ and $Si_2As_2^-$ species, the partially bonding MOs are delocalized on P(3)–P(4) and As(3)–As(4) bonds, respectively. For the most stable $Ge_2N_2^-$ $Ge_2P_2^-$ and $Ge_2As_2^-$ species, the HOMO-3 ($4a_1$) is the partially MO and delocalized on N(3)– N(4), P(3)–P(4) and As(3)–As(4) bonds, respectively.

In order to compare the MOs with the most stable isomer for $X_2Y_2^-$ species, we present delocalized MOs of less stable $X_2Y_2^-$ isomer. As exhibited in Fig. 2(c), the partially bonding MO [HOMO-6 ($3a_1$)] for the less stable $C_2N_2^-$

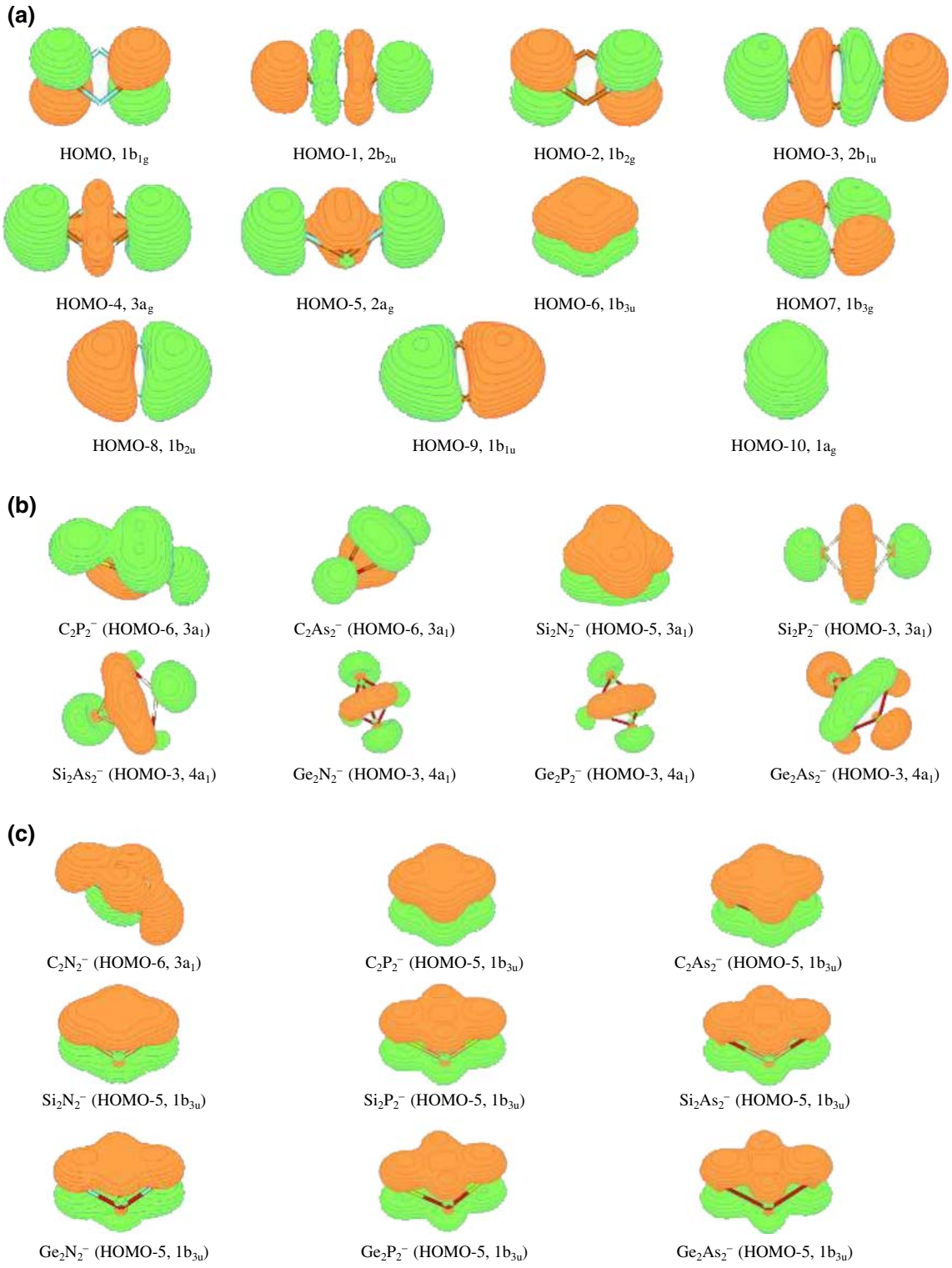

Fig. 2 (a) Molecular orbital (MO) pictures of the most stable $C_2N_2^-$, (b) delocalized π MOs of the most stable $C_2P_2^-$, $C_2As_2^-$, $Si_2N_2^-$, $Si_2P_2^-$, $Si_2As_2^-$, $Ge_2N_2^-$, $Ge_2P_2^-$, $Ge_2As_2^-$, (c) delocalized π MOs of less stable $X_2Y_2^-$ isomer at the B3LYP/6-311 +G* level of theory

isomer is delocalized on N(3)–N(4) bond. For other less stable $X_2Y_2^-$ isomers, the HOMO-5 ($1b_{3u}$) is the partially bonding MO and delocalized on the whole plane of these lesser structures. In the light of the above MO analysis, we can conclude that the existence of delocalized MO for stable isomers of $X_2Y_2^-$ species strengthens the structural stability and make these species show strong aromatic character.

Conclusions

The equilibrium geometries, energies, and harmonic vibrational frequencies of anions $X_2Y_2^-$ (X = C, Si, Ge and Y = N, P, As) clusters are computed and discussed in this paper. Based on these calculations and analysis, it is found that for $C_2N_2^-$ species, the D_{2h} isomer is the most stable four-membered structure, and for other species the C_{2v} isomer in which two X atoms are contrapuntal is the most stable structure at the B3LYP/6-311 +G* level. Wiberg bond index (WBI) and nucleus-independent chemical shift (NICS) values indicate the existence of delocalization in these systems. A detailed molecular orbital (MO) analysis further reveals that a delocalized π MO in occupied molecular orbitals formed from the out-of-plane p orbitals renders π aromaticity to stable $X_2Y_2^-$ structures, which does agree well with the (4n+2) Huckel rule.

Acknowledgments This work was supported by the 111 Project B07012 of China and the National Natural Science Foundation of China No. 20773014.

References

1. Chen ZF, Wannere CS, Corminboeuf C et al. (2005) Chem Rev 105:3842–3888
2. Wodrich MD, Corminboeuf C, Park SS et al. (2007) Chem Eur J 13:4582–4593
3. Kuznetsov AE, Birch K, Boldyrev AI et al. (2003) Science 300:622–625
4. Chi XX, Li XH, Chen XJ et al (2004) THEOCHEM 677:21–27
5. Tsipis CA, Karagiannis EE, Kladou PF et al. (2004) J Am Chem Soc 126:12916–12929
6. Kuznetsov AE, Boldyrev AI (2004) Chem Phys Lett 388:452–456
7. Zhan CG, Zheng F, Dixon DA (2002) J Am Chem Soc 124:14795–14803
8. Elliott BM, Boldyrev AI (2005) J Phys Chem A 109:236–239
9. Corminboeuf C, Heine T, Seifert (2004) J Phys Chem Chem Phys 6:273–276
10. Xu WG, Jin B (2005) THEOCHEM 731:61–66
11. Heine T, Schleyer PvR, Corminboeuf C et al (2003) J Phys Chem A 107:6470–6475
12. Fallah H, Wannere C, Corminboeuf C et al (2006) Org Lett 8:863–866
13. Shetty S, Kanhere DG, Pal SJ (2004) Phys Chem A 108:628–631
14. Li QS, Cheng LP (2003) J Phys Chem A 107:2882–2889
15. Todorov I, Sevov SC (2004) Inorg Chem 43:6490–6494
16. Alexandrova AN, Boldyrev AI, Zhai HJ et al. (2003) J Phys Chem A 107:1359–1369
17. Elliott BM, Boldyrev AI et al (2005) J Phys Chem A 109:236–239
18. Chandrasekhar J, Jemmis ED, PvR S (1979) Tetrahedron Lett 20:3707
19. Zubarev DY, Averkiev BB, Zhai HJ et al. (2008) Phys Chem Chem Phys 10:257–262
20. Zhao J, Balbuena PB (2008) J Phys Chem C 112:3482–3488
21. Xu WG, Jin B (2006) Chem Phys Lett 419:439–443
22. Fowler PW, Rogowska A, Soncini A et al. (2006) J Org Chem 71:6459–6467
23. Alexandrova AN, Boldyrev AI (2003) J Phys Chem A 107:554–560
24. Mallajosyula S, Datta A, Pati SK (2006) J Phys Chem B 110:20098–20101
25. Nigam S, Majumder C, Kulshreshtha SK (2005) THEOCHEM 755:187–194
26. Seo DK, Corbett JD (2001) Science 291:841–842
27. Juselius J, Straka M, Sundholm D (2001) J Phys Chem A 105:9939–9944
28. Mercero JM, Ugalde JM (2004) J Am Chem Soc 126:3380–3381
29. Kleinpeter E, Koch A (2008) THEOCHEM 851:313–318
30. Alkorta I, Blanco F (2008) THEOCHEM 851:75–83
31. Boldyrev AI, Kuznetsov AE (2002) Inorg Chem 41:532–537
32. Schleyer PvR, Maerker C, Dransfeld A et al (1996) J Am Chem Soc 118:6317–6318
33. Li X, Kuznetsov AE, Zhang HF et al (2001) Science 291:859–863
34. Li X, Zhang HF, Wang LS et al (2001) Chem Int Ed 40:1867–1870
35. Kuznetsov AE, Boldyrev AI, Li X et al. (2001) J Am Chem Soc 123:8825–8831
36. Kuznetsov AE, Corbett JD, Wang LS et al (2001) Angew Chem, Int Ed 40:3369–3374
37. Satpati P, Sebastian KL (2008) Inorg Chem 47:2098–2103
38. Gay LJ (1815) Ann Chim 95:175–179
39. Does TV, Bickelhaupt F (1988) Angew Chem, Int Ed Engl 27:936–941
40. Frisch MJ, Trucks GW, Schlegel HB, Scuseria GE, Robb MA, Cheeseman JR, Zakrzewski VG, Montgomery JJA, Stratmann RE, Burant JC, Dapprich S, Millam JM, Daniels AD, Kudin KN, Strain MC, Farkas O, Adamo JC, Clifford S, Ochterski J, Petersson GA, Ayala PY, Cui Q, Morokuma K, Malick DK, Rabuck AD, Raghavachari K, Foresman JB, Cioslowski J, Ortiz JV, Baboul AG, Stefanov BB, Liu G, Liashenko A, Piskorz P, Komaromi I, Gomperts R, Martin RL, Fox DJ, Keith T, Al-Laham MAl, Peng CY, Nanayakkara A, González C, Challacombe M, Gill PMW, Replogle BGES, Pople JA (2003) Gaussian 03. Gaussian Inc, Pittsburgh PA
41. Lin YC, Sundholm D (2006) J Chem Theory Comput 2:761–764
42. Becke AD (1993) J Chem Phys 98:5648–5652
43. Perdew JP, Wang Y (1992) Phys Rev B 45:13244–3249
44. Frisch MJ, Gordon MH, Pople JA (1990) Chem Phys Let 166:275–279
45. Frisch MJ, Gordon MH, Pople JA (1990) Chem Phys Lett 166:281–285
46. Reed AE, Curtiss L, Weinhold AF (1988) Chem Rev 88:899–926
47. Ditchfield R (1974) Mol Phys 27:789–807